Proceedings of the 2014 IEEE
International Conference on Robotics and Biomimetics
December 5-10, 2014, Bali, Indonesia

A New Circular-Guided Remote Center of Motion Mechanism for Assistive Surgical Robots

Hiu Man Yip, Peng Li, David Navarro-Alarcon, Zerui Wang, and Yun-hui Liu

Abstract— **Remote center of motion (RCM) mechanisms are widely used in surgical robots to mechanically constrain the position of a certain point in the operation space. Examples of well-known RCM mechanisms include parallelogram mechanisms, spherical linkages, circular guiding arcs, etc. In this paper, a reinforced circular-guided RCM mechanism is presented. In the mechanism, a closed-looped circular-guiding arc instead of an open-looped one is used to improve rigidity. In addition, with this linearly-actuated RCM mechanism, we can avoid moving the actuator along with its link. This provides an alternative to the use of tendon-driven mechanisms. The proposed mechanism is then further extended to a 3-degree-of-freedom (DOF) configuration for surgical robots. In contrast to most applications where the RCM is designed to be placed out of the patient's body, our new RCM is designed to be placed inside body, which is more preferable in some applications, for example, uterus positioning during laparoscopic hysterectomy. In this paper, the design, dynamic model, static analysis and the extended application of the linearly-actuated-arc-guided RCM mechanism is presented. A prototype is built to validate the feasibility of the mechanism and experiments are conducted.**

I. INTRODUCTION

Remote center of motion (RCM) mechanism is widely used in surgical robots to mechanically constrain the motion of a point to improve safety of the robotic system [1]. Examples of RCM mechanism include but not limited to parallelogram mechanism (e.g. [2]), spherical linkages (e.g. [3], [4]) and circular guiding arcs (e.g. [5], [6]).

A. Motivation

For RCM mechanisms, the size of the system generally varies according to the distance between the desired RCM location and the robot links needed, the longer the required distance, the larger the system would be. For example, for a circular-guided RCM mechanism, the farer the RCM is required, the larger the radius of the guiding arc is needed.

Having a large mechanical structure results in a heavy robot with large footprint. The larger the footprint of the robot, the more space it occupies, which leads to the result that the robot obstructs the surgeons and other medical staff in the operating theater. This prevent the surgeon from working side by side with the robot, which is not preferable for an assistive surgical robot. For example, when using the DaVinci Surgical System, the surgeon has to control the robot through a control console which is distant from the operating table as well as the patient [7]. Besides, a heavy robot has less mobility, i.e. moving the robot around the operating room would become more difficult as the weight of the robot increases. The large inertia of the robot would also make it hard to be stopped by the user once accident occurs.

Reducing the weight of a large mechanical system without modifying its structure may result in weak structure. Weak structure may reduce the rigidity of the system and cause more vibration. Eventually, the reliability and performance of the system can be affected.

Thus, improving the rigidity of the system while keeping the system's size and weight is an important issue to deal with when building compact assistive surgical robots.

B. Related Works

Surgical robots which attain an RCM by using a circular guiding arc include Viky [8], [9] and Probot [10]. Though using a circular guiding arc to attain an RCM is a intuitive way to achieve so, robots built with such mechanism may have the problem of the actuator has to move along the link in order to give the motion [11] or the circular arc itself has to move during the motion, this may reduce the stability of the system and cause difficulties in cabling. In addition, this mechanism may also lead to the existence of an open-looped arc structure [12] which increases the chance of having vibration and thus reduces the stability and reliability of the robot.

In [13], Tang et al. proposed an RCM mechanism which aims at improving the rigidity of RCM mechanisms. With this mechanism, the open-looped structure is eliminated and rigidity of the system can be improved. However, the relative distance between the end-effector (i.e. the instrument's tip) and the RCM keeps changing during the robot's motion, which is not desired in the application of surgical tool manipulation. If the relative distance between the end-effector and the RCM has to be kept constant, an extra degree of freedom for active motion compensation will be needed, which increases the cost and control complexity of the system.

For parallelogram mechanisms, it is common that the link of the system intersects with the axis of the RCM (e.g. [14], [15]), this gives limitation to the system when it is applied to cases that such space is not allowed. For example, when performing uterus positioning during laparoscopic hysterectomy, it is more preferable to place the RCM at the patient's cervix, but, there exist no space to accommodate any part of the robot under the operating table.

Research supported by the ITF of HKSAR under the grant ITS/020/12FP.

Hiu Man Yip, Peng Li, David Navarro-Alarcon, Zerui Wang and Yun-hui Liu are with the Department of Mechanical and Automation Engineering, The Chinese University of Hong Kong, Shatin N.T., Hong Kong S.A.R. (e-mail: hmyip@mae.cuhk.edu.hk)

978-1-4799-7397-2/14/$31.00 © 2014 IEEE

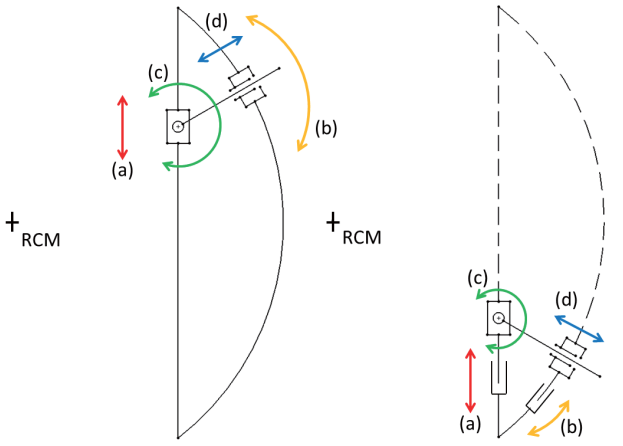

Fig. 1. Schematic diagram of the linearly-actuated-arc-guided RCM mechanism with closed-loop design.

C. Contribution

In this paper, we present a linearly-actuated-arc-guided RCM mechanism which reinforces the traditional circular-guiding arc RCM mechanism. The mechanism provides an alternative to tendon-driven mechanism and avoid the actuator from moving along its link. In addition, open-looped circular-arc structure is naturally eliminated along with this mechanism, which improves the rigidity. Furthermore, the mechanism is extended to a 3-degree-of-freedom (DOF) one for applying to surgical robots which an in-body RCM is more preferable. To validate the feasibility, a prototype is built and experiments are conducted.

II. DESIGN OF MECHANISM

In this section, the design of the linearly-actuated-arc-guided RCM mechanism is presented. The goal and objectives of the mechanism are as follow:

- To output a circular trajectory with the RCM located at the center of the circular trajectory.
- To allow the actuator to be installed on link i without using a tendon driven mechanism. (i.e. if the mechanism is the only DOF of the robot, the actuator would be installed on the base of the robot.)
- To improve the rigidity of a circular-guided RCM mechanism by eliminating the open-ended circular guide structure.

The schematic diagram of the mechanism is shown in Fig. 1. The figure shows the two configurations of the mechanism. In general, the mechanism consists of four components, one active component (a) and three passive components (b-d).

Consider the model on the left side of Fig. 1. The actuated prismatic joint is denoted by (a); the actuator (e.g. a motor) is installed to drive this joint so that the block is driven to move along the vertical axis. The output joint, which is a passive element, is denoted by (b); Element (b) is forced to roll along an arc-shaped guide and gives a circular trajectory with the RCM located at the center of the circular trajectory. To drive the passive output joint (b), connection between the actuated prismatic joint (a) and the output sliding joint (b) is necessary. As elements (a) and (b) are moving in two different trajectories, to connect (a) and (b) without disabling their motions, compensations for the relative angle and distance between these elements are needed. In the mechanism, a revolute joint (c) and a prismatic joint (d) is used for motion compensation between (a) and (b). Both (c) and (d) are unactuated.

In general applications of surgical tool manipulation during minimally invasive surgery (MIS), the surgical tool (considered as a straight rod) should lie on the normal of the arc-shaped guide and pass through the RCM. In addition, the relative distance between the end of the surgical tool and the tangent of the arc-shaped guide should remain constant. This can be achieved by mounting the surgical tool to the output sliding link (b). With this configuration, the relative distance between the tip of the surgical tool and the RCM of the mechanism can keep constant without any extra active motion compensation.

In Fig. 1, the model on the right side shows a variation of the mechanism, the two models in Fig. 1 are equivalent. In this configuration, (a) remains a actuated prismatic joint and the passive revolute joint (c) and prismatic joint (d) for motion compensation shows no modification. Here, modification is done to the driven output joint (d). In the original model on the left, (b) contains an element rolling along an arc-shaped guide rail, here, (b) is modified to a prismatic joint moving along a circular trajectory instead of a linear one. By doing so, the structure on the top (indicated with a dotted line) can be eliminated while naturally keeping the mechanism in the form of a closed loop.

To prove that the mechanism can be driven by one actuator, mobility (i.e. the number of DOFs) of the mechanism is verified with the Grubler's equation [16]:

$$M = 3(L-1) - 2J \tag{1}$$

where M is the mobility (i.e. DOF), L is the number of links and J is the number of joints in the mechanism. It can be observed that there are four links and four joints in the mechanism, thus the mobility equals one and the mechanism can be driven by one actuator.

III. THE EXTENDED 3-DOF RCM MECHANISM

In general applications, one degree of freedom is not enough for a surgical robot. In this section, we extend the mechanism to a 3-DOF one which enables yaw, pitch and insertion motions. This 3-DOF mechanism can be applied to a robot assistant which assists in uterus positioning during laparoscopic hysterectomy [17]. When applying to laparoscopic hysterectomy, the 3-DOF in this mechanism enables anteversion/retroversion of uterus, lateral manipulation of uterus and tensioning of uterus. Fig. 2 shows the schematic diagram of the extended 3-DOF RCM mechanism.

In this mechanism, the linearly-actuated-arc-guided mechanism presented in the above section provides the pitch motion. Here, we denote this joint which provides pitch

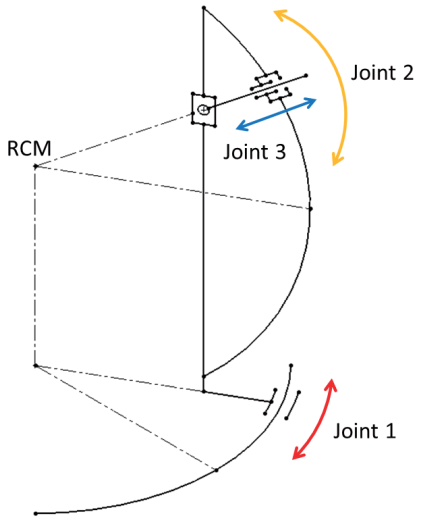

Fig. 2. Schematic diagram of the extended 3-DOF RCM mechanism.

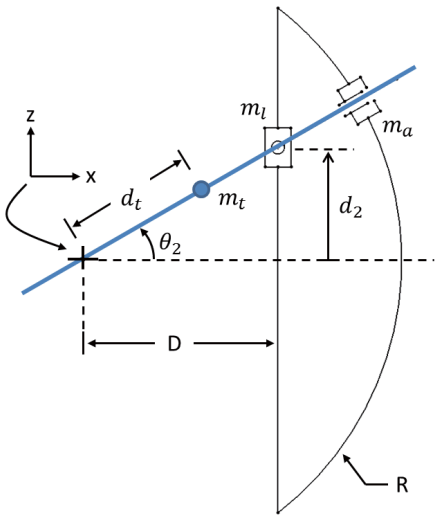

Fig. 3. Parameters of the RCM mechanism.

motion as joint 2. Denote the structure that the output element of joint 2 moves along (i.e. the arc guide) by link 2. Link 2 is designed to move along a circular-guide (i.e. the base link) parallel to the xy-plane, this enables the yaw motion. Here, we denote this joint by joint 1. Denote the output element of joint 2 by link 3. On link 3, a prismatic joint is introduced to enable insertion, we denote it by joint 3.

To make this 3-DOF mechanism share the same RCM, the following requirements have to be fulfilled:

- The axis of rotation of the yaw joint must intersect the RCM of the output trajectory of the linearly-actuated-arc-guided mechanism.
- The axis of translation of the insertion joint must lie on the normal of the output trajectory of the linearly-actuated-arc-guided mechanism and pass through its RCM.

From Fig. 2, it can be observed that by arranging the mechanism in such configuration, interference between the links of the robot and the vertical axis passing the RCM is avoided. This solves the installation problem when the space along this axis is not available for accommodating the robot.

IV. DYNAMIC MODEL AND STATIC ANALYSIS

In this session, we derive the dynamic model of the new RCM mechanism. The dynamic equation of the linearly-actuated-arc-guided RCM mechanism can be derived by the Lagrangian method [18]. In the derivation, we assume the mechanism is composed of three components, a point mass which moves along a vertical trajectory, a point mass which moves along a arc-shaped trajectory, and a rigid rod (i.e. the surgical tool) mounted to the point mass moving along the arc-shaped trajectory. The masses of these components are denoted by m_l, m_a and m_t respectively and the moment of inertia of the the rigid rod is denoted by I_t. Parameters of the mechanism are indicated as shown in Fig. 3. In the figure, the blue line represents the surgical tool mounted to the system.

Note that the presented analysis only considers the linearly-actuated RCM mechanism, therefore, we assume that the other joints in the extended 3-DOF RCM mechanism are static.

As the mechanism is a 1-DOF system, the generalized coordinate can be expressed by $\mathbf{q} = \{d_2\}$, where d_2 is the displacement of the point mass moving vertically. Position vectors of the components can then be written as follow:

$$\mathbf{r}_l = \begin{bmatrix} D & 0 & d_2 \end{bmatrix}^\top \tag{2}$$

$$\mathbf{r}_a = \begin{bmatrix} R\cos\theta_2 & 0 & R\sin\theta_2 \end{bmatrix}^\top \tag{3}$$

$$\mathbf{r}_t = \begin{bmatrix} d_t\cos\theta_2 & 0 & d_t\sin\theta_2 \end{bmatrix}^\top \tag{4}$$

where $\theta_2 = \tan^{-1}(\frac{d_2}{D})$, D is the distance between the RCM and the linear guide, R is the radius of the guiding arc, d_t is the distance between the RCM and the center of mass of the rigid rod, $\mathbf{r}_l$, $\mathbf{r}_a$ and $\mathbf{r}_t$ are the position vectors of the point masses m_l, m_a and the center of mass of the rigid rod respectively.

With the position vectors, the velocities of the components can be calculated by differentiation and hence their kinetic and potential energies can be calculated. The Lagrangian can then be obtained using the total kinetic and potential energies by:

$$L = K - U \tag{5}$$

where L is the Lagrangian, K is the kinetic energy of the system and U is the potential energy of the system. The detailed Lagrangian expression of our mechanism can be found in Appendix A.

Assume no external force is applied to the system, then, the dynamic equation of the mechanism can be calculated by:

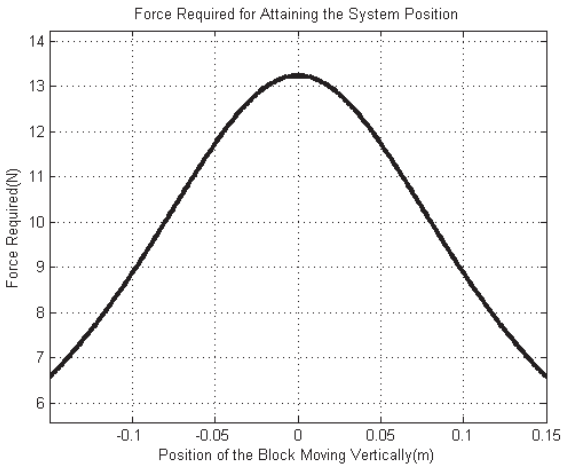

Fig. 4. Force required to maintain the position of the mechanism in static state.

$$u_2 = \frac{d}{dt}(\frac{\partial L}{\partial \dot{d_2}}) - \frac{\partial L}{\partial d_2} \tag{6}$$

where u_2 is the driving torque of the mechanism, t is the time variable and $\dot{d_2}$ is the time derivative of d_2. Details of the dynamic equation of our mechanism is presented in Appendix B.

Consider static condition, i.e. all velocities and accelerations are assumed to be zero, the force required to maintain the position of the mechanism is calculated. Here, we assume $D = 0.15m$, $R = 0.225m$, $d_t = 0.1m$, $I_t = 0.009429kgm^2$, $m_l = 0.3kg$, $m_a = 0.5kg$, $m_t = 0.45kg$ and the acceleration of gravity $g = 9.8ms^{-2}$. We varies d_2 from $-0.15m$ to $0.15m$, the resulting plot is as shown in Fig. 4.

From the result, it can be observed that if an actuation mechanism without self-locking property is implemented to drive the vertically moving component, the mechanism is back-drivable. Furthermore, the force required to maintain the arc-guided block in the horizontal position is the highest while the required force decreases while the block moving towards the two ends. This explains that the mechanism is more back-drivable in the middle region as larger force is required to retain its position. On the contrary, when the arc-guided block moves towards the two ends, less force is required to retain its position, that is, the block has the tendency in staying at its position, thus back-drivability decreases.

V. THE PROTOTYPE

A prototype is built to validate the feasibility of the presented linearly-actuated-arc-guided mechanism. Fig. 5(a) shows the system. In the prototype, the actuated linear joint is realized by a belt-and-pulley mechanism. A 20W DC motor is used as the actuator. From the figure, it is observed that the motor is installed on link i of the system. For the output joint, it consists of a block rolling along a smooth arc-shaped rail, this helps in obtaining a smoother joint motion.

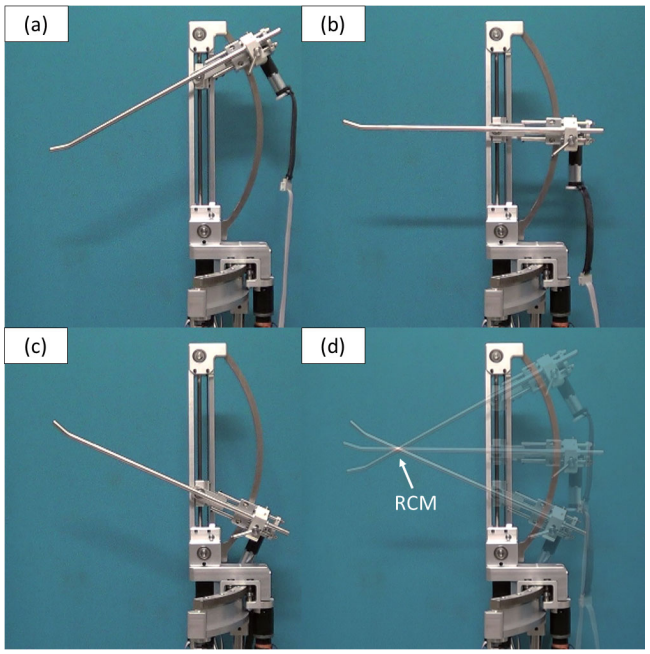

Fig. 5. The existence of an RCM. (a)-(c) shows the frames of the video captured. (d) shows the result after overlapping frames (a) to (c).

To verify that the mechanism does have the ability to move with an RCM, a video is recorded. When recording the video, the camera is fixed to a tripod, this is to ensure that the viewpoint is fixed. Then, power is given to the actuator and the motion of the prototype is observed. Here, a uterus manipulator (with shape of a rod with an up-tilting tip) is used as the surgical tool [19]. The existence of an RCM is proved by overlapping the frames of the video captured (Fig. 5). In Fig. 5, (a) to (c) show the frames from the video and (d) shows the result after overlapping frame (a) to (c). It can be observed that no matter how the joints move, there exists a common point that the surgical tool always passes through despite of the orientation of the tool. This common point is the RCM of the mechanism, which is a stationary point that does not affected by all joint motions of the mechanism.

Similar videos have been recorded to verify the existence of an RCM in the extended 3-DOF mechanism. The results are shown in Fig. 6 and Fig. 7. In both figures, (a) is used as a reference, which joint 2 is moved. In Fig. 6, (b) and (c) show the movements of joint 1 while the movement of joint 3 is shown in (b) and (c) of Fig. 7. The results after overlapping (a) to (c) is shown in (d). It can be observed that no matter how the joints move, there exists a stationary point, which is the RCM.

VI. CONCLUSIONS

In this paper, a linearly-actuated-arc-guided RCM mechanism aimed at reinforcing the circular-guided RCM mechanism is presented. Apart from improving rigidity, this mechanism provides the advantage of avoiding the actuator from moving along the link without using a tendon-driven mechanism, this gives an alternative for the choice of mechanism. Design of the mechanism is provided and the mechanism is

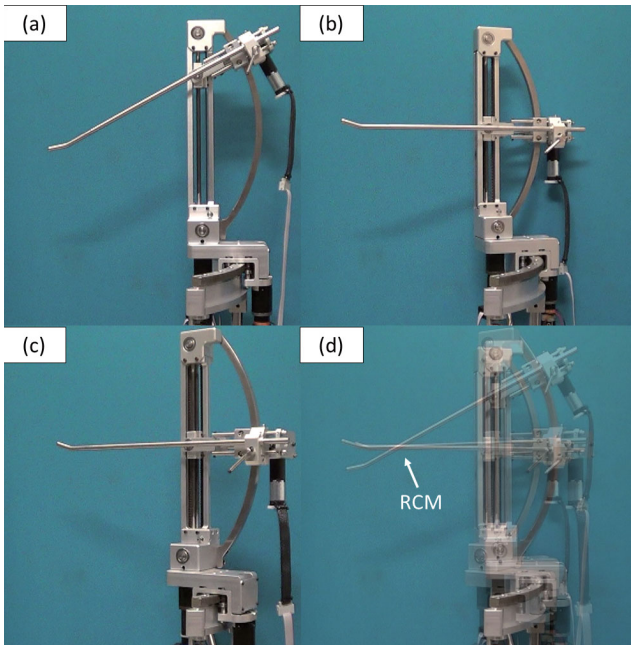

Fig. 6. The existence of an RCM. (a) shows the motion of joint 2 as a reference and (b)-(c) shows the movement of joint 1. (d) shows the result after overlapping frames (a) to (c).

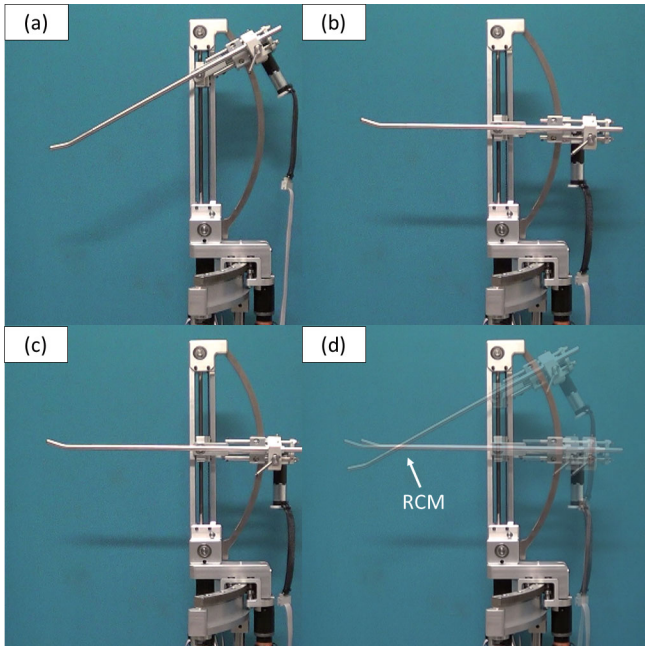

Fig. 7. The existence of an RCM. (a) shows the motion of joint 2 as a reference and (b)-(c) shows the movement of joint 3. (d) shows the result after overlapping frames (a) to (c).

further extended to a 3-DOF one with the same RCM. The dynamics and statics of the system are analysed. From the result, it is shown that the mechanism is back-drivable and the back-drivability is the highest when the output joint is at the horizontal position. With the prototype built based on the presented design, it is proved that the mechanism is feasible and a remote center of motion is obtained.

It is expected that the mechanism can be applied to the development of assitive surgical robots in the near future, for example, a robotic system for uterus positioning during laparoscopic hysterectomy. In addition, passive safety mechanisms are suggested to be integrated to the prototype to make the system more appropriate for medical purposes. For example, passive safety mechanism which limits the interaction force between the surgical tool and the patient can implemented to the system to protect the patient from injury.

APPENDIX A

The expression of the Lagrangian of the linearly-actuated-arc-guided mechanism is as follow:

$$\begin{aligned} L = {} & \frac{m_a}{2}\left[\frac{R\dot{d_2}}{(D(\frac{d_2^2}{D^2}+1)^{\frac{1}{2}}} - \frac{Rd_2^2\dot{d_2}}{D^3(\frac{d_2^2}{D^2}+1)^{\frac{3}{2}}}\right]^2 + \frac{m_l\dot{d_2}^2}{2} \\ & + \frac{m_t}{2}\left[\frac{d_t\dot{d_2}}{D(\frac{d_2^2}{D^2}+1)^{\frac{1}{2}}} - \frac{d_td_2^2\dot{d_2}}{D^3(\frac{d_2^2}{D^2}+1)^{\frac{3}{2}}}\right]^2 - gm_ld_2 \\ & + \frac{I_t\dot{d_2}^2}{2D^2(\frac{d_2^2}{D^2}+1)^2} - \frac{d_tgm_td_2}{D(\frac{d_2^2}{D^2}+1)^{\frac{1}{2}}} + \frac{R^2m_ad_2^2\dot{d_2}^2}{2D^4(\frac{d_2^2}{D^2}+1)^3} \\ & + \frac{d_t^2m_td_2^2\dot{d_2}^2}{2D^4(\frac{d_2^2}{D^2}+1)^3} - \frac{Rgm_ad_2}{D(\frac{d_2^2}{D^2}+1)^{\frac{1}{2}}} \end{aligned} \tag{7}$$

where g is the acceleration of gravity.

APPENDIX B

The dynamic equation of the linearly-actuated-arc-guided mechanism is as follow:

$$u_2 = H(\mathbf{q})\ddot{d_2} + C(\mathbf{q},\dot{\mathbf{q}}) + G(\mathbf{q}) \tag{8}$$

where $\ddot{d_2}$ is the second time derivative of d_2 and

$$H(\mathbf{q}) = m_l + \frac{D^2(m_aR^2 + m_td_t^2 + I_t)}{(D^2+d_2^2)^2} \tag{9}$$

$$C(\mathbf{q},\dot{\mathbf{q}}) = -\frac{2D^2d_2\dot{d_2}^2(m_aR^2 + m_td_t^2 + I_t)}{(D^2+d_2^2)^3} \tag{10}$$

$$\begin{aligned} G(\mathbf{q}) = {} & gm_l - \frac{g}{(D^2+d_2^2)^4}[D^5Rd_2^2m_a(\frac{d_2^2}{D^2}+1)^{\frac{5}{2}} \\ & + D^5d_2^2d_tm_t(\frac{d_2^2}{D^2}+1)^{\frac{5}{2}} - D^7Rm_a(\frac{d_2^2}{D^2}+1)^{\frac{7}{2}} \\ & + D^7d_tm_t(\frac{d_2^2}{D^2}+1)^{\frac{7}{2}}] \end{aligned} \tag{11}$$

REFERENCES

[1] C.-H. Kuo and J. Dai, "Robotics for minimally invasive surgery: a historical review from the perspective of kinematics," in *International Symposium on History of Machines and Mechanisms*, H.-S. Yan and M. Ceccarelli, Eds. Springer Netherlands, 2009, pp. 337–354.

[2] A. Madhani, G. Niemeyer, and J. Salisbury, "The black falcon: a teleoperated surgical instrument for minimally invasive surgery," in *Intelligent Robots and Systems, 1998. Proceedings., 1998 IEEE/RSJ International Conference on*, Oct. 1998, pp. 936–944 vol.2.

[3] N. Zemiti, G. Morel, T. Ortmaier, and N. Bonnet, "Mechatronic design of a new robot for force control in minimally invasive surgery," *Mechatronics, IEEE/ASME Transactions on*, vol. 12, no. 2, pp. 143–153, 2007.

[4] J. Rosen, M. Lum, M. Sinanan, and B. Hannaford, "Raven: developing a surgical robot from a concept to a transatlantic teleoperation experiment," in *Surgical Robotics*, R. M. S. Jacob Rosen, Blake Hannaford, Ed. Springer, 2011, pp. 159–197.

[5] Hyosig Kang and Wen, J.T., "Robotic assistants aid surgeons during minimally invasive procedures," *Engineering in Medicine and Biology Magazine, IEEE*, vol. 20, pp. 94–104, Jan. 2001.

[6] Buess GF, Arezzo A, Schurr MO, Ulmer F, Fisher H, Gumb L, Testa T, Nobman C., "A new remote-controlled endoscope positioning system for endoscopic solo surgery. the fips endoarm," *Surg Endoscopy*, vol. 24, pp. 395–399, Apr. 2000.

[7] G. Guthart and J. Salisbury, J., "The intuitivetm telesurgery system: overview and application," in *Robotics and Automation, 2000. Proceedings. ICRA '00. IEEE International Conference on*, 2000, pp. 618–621 vol.1.

[8] P. Berkelman and J. Ma, "A compact modular teleoperated robotic system for laparoscopic surgery," *The International Journal of Robotics Research*, vol. 28, pp. 1198–1215, 2009.

[9] P. Berkelman, E. Boidard, P. Cinquin, and J. Troccaz, "Ler: the light endoscope robot," in *Intelligent Robots and Systems, 2003. (IROS 2003). Proceedings. 2003 IEEE/RSJ International Conference on*, Oct. 2003, pp. 2835–2840 vol.3.

[10] S. Harris, Q. Mei, R. Hibberd, and B. Davies, "Experiences using a special purpose robot for prostate resection," in *Advanced Robotics, 1997. ICAR '97. Proceedings., 8th International Conference on*, July 1997, pp. 161–166.

[11] J. Long, P. Cinquin, J. Troccaz, S. Voros, P. Berkelman, J. Descotes, C. Letoublon, and J. Rambeaud, "Development of miniaturized light endoscope-holder robot for laparoscopic surgery," *Journal of Endourology*, vol. 21, pp. 911–914, 2007.

[12] H. M. Yip, P. Li, and Y. Liu, "Design and development of a robotic assistant for uterus manipulation in total laparoscopic hysterectomy," in *Information and Automation (ICIA), 2014 IEEE International Conference on*, July 2014.

[13] H.-W. Tang, H. van Brussel, J. Peirs, and T. Janssens, "Remote centre of motion positioner," Patent US20 120 132 018 A1, May 31, 2012.

[14] R. Taylor, J. Funda, B. Eldridge, S. Gomory, K. Gruben, D. LaRose, M. Talamini, L. Kavoussi, and J. Anderson, "A telerobotic assistant for laparoscopic surgery," *Engineering in Medicine and Biology Magazine, IEEE*, vol. 14, no. 3, pp. 279–288, 1995.

[15] P. Li, H. M. Yip, D. Navarro-Alarcon, Y. Liu, C. Tong, and I. Leung, "Development of a robotic endoscope holder for nasal surgery," in *Information and Automation (ICIA), 2013 IEEE International Conference on*, Aug. 2013, pp. 1194–1199.

[16] R. L. Norton, *Design of Machinery*: *An Introduction to the Synthesis and Analysis of Mechanisms and Machines*. McGraw-Hill Higher Education, 1999, p. 29.

[17] H. M. Yip, P. Li, D. Navarro-Alarcon, and Y. hui Liu, "Towards developing a robot assistant for uterus positioning during hysterectomy: system design and experiments," *Robotics and Biomimetics*, to be published.

[18] J. J. Craig, *Introduction to Robotics*: *Mechanics and Control, Third Edition*. Pearson Education, 2005, pp. 182–183.

[19] C. Ng and B. Chern, "Total laparoscopic hysterectomy: a 5-year experience," *Archives of Gynecology and Obstetrics*, vol. 276, pp. 613–618, 2007.